LUND UNIVERSITY

Mathematical modeling and statistical analysis of calcium-regulated insulin granule exocytosis in beta-cells from mice and humans.

Pedersen, Morten Gram; Cortese, Giuliana; Eliasson, Lena

Link to publication

Total number of authors:
3

Mathematical modeling and statistical analysis of calcium-regulated insulin granule exocytosis in β-cells from mice and humans

Morten Gram Pedersen[a,c], Giuliana Cortese[b], Lena Eliasson[a]

[a]*Islet Cell Exocytosis, Lund University Diabetes Centre, Department of Clinical Sciences, Clinical Research Centre, Lund University, CRC 91-11, UMAS entrance 72, SE-20502 Malmö, Sweden. E-mail:* `morten_gram.pedersen@med.lu.se, lena.eliasson@med.lu.se`
[b]*Department of Biostatistics, University of Copenhagen, Øster Farimagsgade 5B, P.O.B. 2099, 1014 Copenhagen K, Denmark. E-mail:* `g.cortese@biostat.ku.dk`
[c] *Corresponding author: M.G. Pedersen, Phone: +46 40 391156, Fax: +46 40 391222.*

Abstract

Insulin is released from pancreatic β-cells as a result of Ca^{2+}-evoked exocytosis of dense-core granules. Secretion is biphasic, which has been suggested to correspond to the release of different granule pools. Here we review and carefully reanalyze previously published patch-clamp data on depolarization-evoked Ca^{2+}-currents and corresponding capacitance measurements. Using a statistical mixed-effects model, we show that the data indicate that pool depletion is negligible in response to short depolarizations in mouse β-cells. We then review mathematical models of granule dynamics and exocytosis in rodent β-cells and present a mathematical description of Ca^{2+}-evoked exocytosis in human β-cells, which show clear differences to their rodent counterparts. The model suggests that L- and P/Q-type Ca^{2+}-channels are involved to a similar degree in exocytosis during electrical activity in human β-cells.

Keywords: Insulin secretion, Large dense-core vesicles, Cell membrane capacitance increase, Ca^{2+} microdomains, Ca^{2+} sensitivity, Mixed-effects model

1. Introduction

The polypeptide insulin is released from pancreatic β-cells at high glucose levels to lower blood-sugar levels by promoting glucose uptake by muscles and adipose tissues in addition to reducing glucose output from the liver. The release of insulin is biphasic; a first rapid phase of secretion is followed by a second phase with slower release (Curry et al., 1968). Prior to release insulin is contained in secretory granules. These granules are transported to the plasma membrane via the microtubules (Varadi et al., 2002; Ivarsson et al., 2004), and actin networks (Ivarsson et al., 2005). At the plasma membrane the granules are docked and primed through Ca^{2+}, temperature- and ATP-dependent processes (Proks et al., 1996; Renström et al., 1996; Eliasson et al., 1997). Ultrastructural analysis (Olofsson et al., 2002) in single mouse β-cells has revealed that $\sim$700 out of the total $\sim$10 000 granules are docked to the plasma membrane. Of these $\sim$200 are primed and readily releasable.

The main pathway of glucose-stimulated insulin secretion is well-established (Ashcroft and Rorsman, 1989; Misler et al., 1992; Henquin, 2000). Glucose enters the β-cell through GLUT glucose transporters and is then metabolized. The resulting increase in the ATP-to-ADP ratio leads to the closure of ATP-sensitive K^+-channels, which allows a leak current to depolarize the plasma membrane and trigger electrical activity. The depolarizations open voltage-dependent Ca^{2+}-channels, and once the intracellular Ca^{2+} concentration increases by influx of Ca^{2+} through the Ca^{2+}-channels (Ammälä et al., 1993b) the granules fuse with the plasma membrane and insulin is released.

The understanding of processes involved in exocytosis of insulin granules has increased tremendously during the last 20 years through the introduction of techniques such as carbon fibre amperometry (Smith et al., 1995), TIRF microscopy (Ohara-Imaizumi et al., 2004), and live confocal imaging (Ivarsson et al., 2004), but also capacitance measurements in combination with the patch-clamp technique (Gillis and Misler, 1992). Using the latter method, we and others have suggested that granules can be divided into different functional pools prior to release [see e.g. Eliasson et al. (2008)]. Granules docked and primed at the plasma membrane belong to the readily releasable pool (RRP). A subset of this pool termed the immediately releasable pool (IRP) is situated in close contact to the L-type Ca^{2+}-channels [$\sim$10 nm distance; Wiser et al. (1999)]. Granules within the IRP are accordingly situated within the Ca^{2+}-channel microdomains. The majority of the granules belong to a reserve pool (RP) and these needs to be transported, docked and primed prior

to release. On a cellular level it has been suggested that first phase insulin secretion is equivalent to release of granules from the IRP/RRP and second phase insulin secretion correspond to the release of granules from the RP (Daniel et al., 1999; Eliasson et al., 2008). Interestingly, first phase insulin secretion is lacking in patients with type 2 diabetes (Hosker et al., 1989) why studies investigating the control of the IRP/RRP is of great importance.

In addition to the triggering pathway described above, an amplifying pathway is acting to augment insulin release (Henquin, 2000). The amplifying pathway is also referred to as the KATP-independent pathway, and it is not activated until the triggering pathway has depolarized the membrane and increased intracellular Ca^{2+}. The amplifying pathway can be investigated under depolarized conditions bypassing the KATP-channel such as when stimulating insulin secretion using high K^{+} in presence of diazoxide (Gembal et al., 1992) or performing patch-clamp capacitance measurements (Gillis and Misler, 1992; Ammälä et al., 1993b) The most known amplifying factors are ATP (Eliasson et al., 1997) and cAMP (Gillis and Misler, 1993; Renström et al., 1997). Other potentiating factors include Malonyl-CoA (Prentki et al., 1992), glutamate (Maechler and Wollheim, 1999) and NADPH (Ivarsson et al., 2005).

The exocytotic response in pancreatic β-cells can also be enhanced by agents such as the incretins glucagon-like peptide-1 (GLP-1) (Gromada et al., 1998) and glucose-dependent insulinotropic polypeptide (GIP) (Ding and Gromada, 1997). These hormones increase the intracellular cAMP-concentration by binding to respective G-protein coupled receptors and activation of adenylate cyclases. Adenylate cyclases can also be activated by the pharmacological compound forskolin to generate cAMP. Potentiation of insulin exocytosis by cAMP involves both activation of protein kinase A (PKA) (Renström et al., 1997) and Epac 2 (Exchange protein associated with cAMP 2) (Ozaki et al., 2000). Using capacitance measurements, we have suggested that PKA stimulates mobilization whereas Epac 2 is involved in rapid exocytosis of IRP/RRP granules (Eliasson et al., 2003). Conditional for rapid cAMP-dependent exocytosis is also the presence of the SNARE-protein SNAP-25, which binds to Epac 2 (Vikman et al., 2009). Epac has further been suggested to bind to piccolo (Fujimoto et al., 2002) and to associate with the plasma membrane sulphonylurea receptor SUR1 (Eliasson et al., 2003).

Here we have carefully reanalyzed previously published data (Eliasson et al., 2003) with attention to the positive effect of forskolin on exocytosis by using a statistical mixed-effects model (Pinheiro and Bates, 2000). We find

3

that the data show a linear relation between depolarization-evoked membrane capacitance increase (ΔC_m) and the Ca^{2+}-charge entering during a depolarization (Q), and argue that this indicates that pool depletion is negligible in response to short depolarizations in mouse β-cells. A mathematical model of exocytosis in human β-cells is also presented. Simulations show that human exocytosis data are well reproduced by assuming that granules fuse away from Ca^{2+}-channels. We find that during electrical activity L- and P/Q-type Ca^{2+}-channels contribute similarly to exocytosis in human β-cells.

Parts of this work has been published previously in abstract form (Pedersen, 2010c).

2. Methods

Capacitance measurements and Ca^{2+}-entry data from mouse β-cells were taken from Eliasson et al. (2003), where details on the experiments are provided. Briefly, using the perforated-patch technique, pulses of increasing length (5-850 ms) were applied to isolated single mouse β-cells, and resulting Ca^{2+}-currents and increases in membrane capacitance were recorded. The data in the absence and presence of 2 μM forskolin was used for the statistical analysis. Ca^{2+}-currents were inspected visually, and data with large leak currents or high amounts of noise were discarded for the analysis.

In a first statistical analysis, we fitted linear models for regression of ΔC_m on Q, taking the differences between cells into account. Because a significant between-cell variation was present within both the control and forskolin-stimulated groups, a second more appropriate analysis was performed by fitting a linear mixed-effects model (Pinheiro and Bates, 2000), with treatment group as fixed effect and cell as random effect, to the data. Mixed-effects models are more appropriate for representing clustered data, such as in our case where several observations are done on each cell. The final model was of the form

$$\Delta C_{m,ij} = (\beta + \beta_{FSK} \cdot FSK_i + b_i)Q_{ij} + \epsilon_{ij}, \quad \epsilon_{ij} \sim N(0,\sigma), b_i \sim N(0,\sigma_b), \quad (1)$$

for observation j of cell i, where ϵ_{ij} is a normally distributed error term, FSK_i is a covariate indicating whether cell i was exposed to forskolin, b_i is a factor allowing for cell-to-cell variation, and the parameters $\beta, \beta_{FSK}, \sigma$ and σ_b are to be estimated. The contrast to traditional modeling lies in the introduction of the mixed-effect via b_i. The statistical software R was used,

4

in particular the `lme` function of the `nlme` R-package (Pinheiro and Bates, 2000). Parameter estimates are given with standard errors and p-values from two-sided t-tests.

The mathematical model for human β-cells was implemented in XPPAUT (Ermentrout, 2002). Computer code for XPPAUT can be downloaded from `http://www.dei.unipd.it/~pedersen`. The calcium fluxes were modeled by a two-compartment model. Calcium flows into a submembrane space through voltage-dependent channels, and diffuses into a general cytosolic compartment. Extrusion of Ca^{2+} from the cell occurs from the submembrane compartment with flux $J_{pmca} + J_{ncx}$, and exchange with the ER happens from the cytosolic compartment with flux $J_{serca} + J_{leak}$. This leads to

$$\frac{dCa_{mem}}{dt} = f(-\alpha I_{Ca}/v_{mem} - B/f_v(Ca_{mem} - Ca_i) - (J_{pmca} + J_{ncx})), \quad (2)$$

$$\frac{dCa_i}{dt} = f(B(Ca_{mem} - Ca_i) - (J_{serca} + J_{leak})). \quad (3)$$

Here $f = 0.01$ is the ratio of free-to-bound Ca^{2+}, $\alpha = 5.18 \cdot 10^{-12} \, \mu mol/s/pA$ changes current to flux, $v_{mem} = 2 \cdot 10^{-13} L$ is the volume of the submembrane compartment, $f_v = v_{mem}/v_{cell} = 0.174$ is the ratio of submembrane-to-cell volume, and $B = 100/s$ describes diffusion between compartments. A relative large submembrane compartment consisting of a shell of depth $\sim$400 nm was used based on Klingauf and Neher (1997), who showed that in the case of sparse Ca^{2+}-channels, the dynamics between channels is corresponds to a shell model at a depth of $\sim 23\%$ of the channel distance. In mouse β-cells the interchannel distance has been estimated to be $1.2 \, \mu m$ (Barg et al., 2001). The value of B was based on v_{mem} and v_{cell} following De Schutter and Smolen (1998), and adjusted slightly to optimize the model behavior.

Fluxes are as follows

$$J_{serca} = J_{serca,\max} Ca_i^2/(K_{serca}^2 + Ca_i^2), \quad (4)$$

$$J_{pmca} = J_{pmca,\max} Ca_{mem}/(K_{pmca} + Ca_{mem}), \quad (5)$$

$$J_{ncx} = J_{ncx,0} Ca_{mem}, \quad (6)$$

with parameters (Chen et al., 2003),

$$J_{serca,\max} = 100 \, \mu M/s, \qquad K_{serca} = 0.27 \, \mu M,$$
$$J_{pmca,\max} = 21 \, \mu M/s, \qquad K_{pmca} = 0.5 \, \mu M,$$
$$J_{leak} = -0.94 \, \mu M/s, \qquad J_{ncx,0} = 18.67 \, s^{-1}.$$

Here, $J_{serca,\text{max}}$ was raised modestly to give reasonable $[Ca^{2+}]_c$ also during rapid bursting (Fig. 4 D-F; $[Ca^{2+}]_c$ not shown).

The whole-cell calcium current is the sum of T-, L- and P/Q-type currents,

$$I_{Ca} = I_{Ca,T} + I_{Ca,L} + I_{Ca,PQ}, \tag{7}$$

modeled as in Pedersen (2010a) based on Braun et al. (2008) as

$$I_{Ca,X} = g_{CaX}\, m_{X,\infty}(V)\, h_X\, (V - V_{Ca}), \qquad X = T, L, PQ, \tag{8}$$

where g_{CaX}, $X = T, L, PQ$, is the whole-cell conductance of the corresponding channel type, and $V_{Ca} = 65$ mV is the Nernst potential for Ca^{2+}. Activation is assumed to be instantaneous and described by

$$m_{X,\infty}(V) = 1/(1 + \exp((V - V_{mX})/n_{mX})), \qquad X = T, L, PQ, \tag{9}$$

while inactivation is assumed not to occur for P/Q-type channels, $h_{PQ} = 1$, and inactivation of T- and L-type currents follow

$$\frac{dh_X}{dt} = \frac{h_{X,\infty}(V) - h_X}{\tau_X}, \qquad X = T, L, \tag{10}$$

with

$$h_{T,\infty}(V) = 1/(1 + \exp((V - V_{hT})/n_{hT})), \tag{11}$$
$$h_{CaL,\infty}(V) = \min\left(1, 1 - [m_{CaL,\infty}(V)(V - V_{Ca})]/57\text{ mV}\right). \tag{12}$$

Parameters for the currents are

$$
\begin{aligned}
g_{CaT} &= 0.5\,\text{nS}, & V_{xT} &= -40\,\text{mV}, & n_{xT} &= -4\,\text{mV}, \\
V_{yT} &= -64\,\text{mV}, & n_{yT} &= 8\,\text{mV}, & \tau_T &= 0.007\,\text{s}, \\
g_{CaPQ} &= 1.7\,\text{nS}, & V_{xPQ} &= -10\,\text{mV}, & n_{xPQ} &= -10\,\text{mV}, \\
g_{CaL} &= 1.4\,\text{nS}, & V_{xL} &= -25\,\text{mV}, & n_{xL} &= -6\,\text{mV}, & \tau_L &= 0.065\,\text{s}.
\end{aligned}
$$

The only change compared to Pedersen (2010a) is that the time-constant of L-type inactiviation is raised to $\tau_L = 65$ ms to reproduce the slowest inactivation time-constant of the whole-cell Ca^{2+}-current (Braun et al., 2008). To convert conductances relative to cell size to absolute conductances, the capacitance of a human β-cell was set to 10 pF (Braun et al., 2008).

In Fig. 4, membrane potential patterns $V(t)$ were simulated independently using a recent model of electrical activity (Pedersen, 2010a) without modifications, or with minor parameter changes (Fig. 4 D-F, see legend for details). The simulated pattern was then used as a driving function in the calcium dynamics and exocytosis model.

3. Results and Discussion

When exocytosis is triggered by opening Ca^{2+}-channels with depolarizing pulses using the voltage-clamp of the patch-clamp technique, the Ca^{2+}-current can be measured during the depolarization, but only the total increase in cell membrane capacitance ΔC_m is obtained, since C_m can not be followed during the depolarization (Lindau and Neher, 1988; Ammälä et al., 1993b; Horrigan and Bookman, 1994). For this reason, depolarizations of different durations are often applied to follow the dynamics of the exocytotic response, assuming that the kinetics of exocytosis is unchanged from pulse to pulse (Ammälä et al., 1993b; Horrigan and Bookman, 1994; Barg et al., 2001; Braun et al., 2008).

In single mouse β-cells, the exocytotic rate is higher for shorter than for longer pulses (Ammälä et al., 1993b; Barg et al., 2001; Eliasson et al., 2003). The drop in the exocytotic rate at sustained depolarizations has been suggested to result either from Ca^{2+}-channel inactivation (Ammälä et al., 1993b; Engisch and Nowycky, 1996) or depletion of a finite pool of immediately releasable granules (Barg et al., 2001; Eliasson et al., 2003). A frequently applied method to relate the evoked exocytotic response and the Ca^{2+}-current, is to plot ΔC_m as a function of the integrated current, i.e. the charge Q that entered during the depolarization (Engisch and Nowycky, 1996; Barg et al., 2001; Eliasson et al., 2003; Vikman et al., 2006).

Inactivation of the Ca^{2+}-current is a result of closure of single Ca^{2+}-channels rather than of a decrease in the single-channel current. If we assume for simplicity that Ca^{2+}-channels are spatially discrete, for a moment disregarding evidence of Ca^{2+}-channel clustering (Barg et al., 2001), then the Ca^{2+}-concentration in microdomains below open Ca^{2+}-channels is constant during the depolarization, but the number of microdomains will decrease as the Ca^{2+}-current inactivates. When exocytosis is associated with Ca^{2+} entry through discrete channels, and in the absence of pool depletion, then ΔC_m and Q will be linearly related (Augustine et al., 1991), since the rate of exocytosis E is proportional to the number of microdomains N (assumed equal to the number of immediately releasable granules), which decreases in parallel with inactivation of the Ca^{2+}-current I_{Ca}. In mathematical terms (where e_{MD} is the exocytotic rate from a single microdomain, i_{Ca} is the single channel current, and $A = e_{MD}/i_{Ca}$)

$$E(t) = e_{MD}N(t) = e_{MD}I_{Ca}(t)/i_{Ca} = AI_{Ca}(t), \qquad (13)$$

so, by integration, $\Delta C_m = AQ$. The slope A is a measure of Ca^{2+}-efficacy, i.e., the capacitance response to a certain amount of Ca^{2+}-influx Q. Channel clustering does not change this conclusion greatly, and pool depletion will show-up as a deviation from linearity in ΔC_m as a function of Q (Pedersen, 2011).

3.1. Mixed-effects analysis of exocytosis in mouse β-cells

In light of the predicted linear relationship between ΔC_m and Q in the absence of pool depletion, we reanalyzed previously published data from Eliasson et al. (2003) obtained with the perforated-patch technique, since the original analysis did not take Ca^{2+}-currents into account and neglected cell-to-cell variation. We are interested in whether forskolin increases the effect of Ca^{2+} on exocytosis, and whether there is any significant deviation from linearity in the relation between ΔC_m and Q.

Analysis of ΔC_m versus Q has previously been performed by pooling data from different cells, for example according to depolarization length (Barg et al., 2001; Vikman et al., 2006; Braun et al., 2008) or other criteria (Moser and Neher, 1997). Such pooling does not take into account natural cell heterogeneity, but assumes that cells are identical. In another approach, data recorded from all cells have been used to investigate the relation between ΔC_m and Q (Brandt et al., 2005), but this analysis neglects that data from different depolarizations applied to the same cell are more strongly correlated than data obtained in different cells, and is likely to overstate the statistical significance of regression coefficients (Venables and Ripley, 2002).

Mixed-effects models (Pinheiro and Bates, 2000) provide the statistical methodology to handle this situation with intra-cellular correlation and random variation due to biological differences between cells. Thus, we consider a fixed effect of Ca^{2+} on exocytosis, which quantifies the "average" Ca^{2+}-efficacy within each group, and we include a random effect to adjust the model for how the individual cell responses deviate from the group average. See Eq. 1 for details. With this kind of analysis it is possible to test statistically whether forskolin increases the efficacy of Ca^{2+} on exocytosis, by testing whether the parameter β_{FSK} is different from zero, while at the same time quantifying the cell heterogeneity by σ_b.

Visual inspection of the raw data (Fig. 1, circles) suggests that the relation between ΔC_m and Q is near-linear in all cells, and the slope of the relation (Ca^{2+}-efficacy) appears to be higher in forskolin-stimulated cells. We estimate that the Ca^{2+}-efficacy (β) is 0.87 ± 0.31 fF/pC (significantly different

8

from zero, p=0.0065) in control cells, while the presence of forskolin increases the Ca^{2+}-efficacy (β_{FSK}) significantly (p<0.0001) by 2.26 ± 0.45 fF/pC, giving a mean Ca^{2+}-efficacy in the forskolin stimulated group ($\beta + \beta_{FSK}$) of 3.13 fF/pC. Between-cell variation in Ca^{2+}-efficacy (random effect) is modeled by a zero-mean normal distribution with estimated standard deviation of 0.69 fF/pC. Interestingly, this variation in Ca^{2+}-efficacy is substantial in comparison to the fixed-effect Ca^{2+}-efficacy in the control and forskolin groups, and underlines that cell heterogeneity must be taken into account, as we did by considering a mixed-effects model. This conclusion is confirmed statistically, since a likelihood-ratio test shows that inclusion of random-effects leads to a significantly better fit to the data (p<0.0001). The random deviations of the cell responses (full lines) from the group responses (dashed lines) is also evident in Fig. 1. Finally, inclusion of a quadratic term Q^2 does not improve the goodness-of-fit significantly, showing that the linear relation between ΔC_m and Q provides a sufficiently good model for our data. Thus, there is no evidence of pool depletion in this data set.

In summary, we find that the cAMP-elevating agent forskolin significantly increases the efficacy of Ca^{2+} on exocytosis, as has been suggested earlier (Ammälä et al., 1993a; Gillis and Misler, 1993). This might be due to an increase in pool size, likely controlled by PKA (Renström et al., 1997), or a direct effect on the exocytotic machinery, likely acting via Epac 2 (Eliasson et al., 2003). However, we find no sign of pool depletion, indicating that previous analyses (Eliasson et al., 2003) underestimated the number of immediately releasable granules.

3.2. Mathematical modeling of granule dynamics in rodent β-cells

Mathematical models of granule pools and insulin secretion go back at least to Grodsky (1972), who explained biphasic insulin secretion and the secretory response to the so-called staircase protocol with a model that in modern terminology includes a reserve pool and an RRP. Readily releasable granules are assumed to have different thresholds with respect to glucose. Once the glucose concentration rises above the threshold of a granule, it releases its content. The assumption of granules having different glucose thresholds has not been confirmed experimentally. Recently, it was argued using an update of Grodsky's model that threshold behavior on the cellular level (Jonkers and Henquin, 2001), rather than on the levels of granules, can explain the staircase experiments (Pedersen et al., 2008). This model was used (Pedersen et al., 2010) to show how cell heterogeneity might underlie
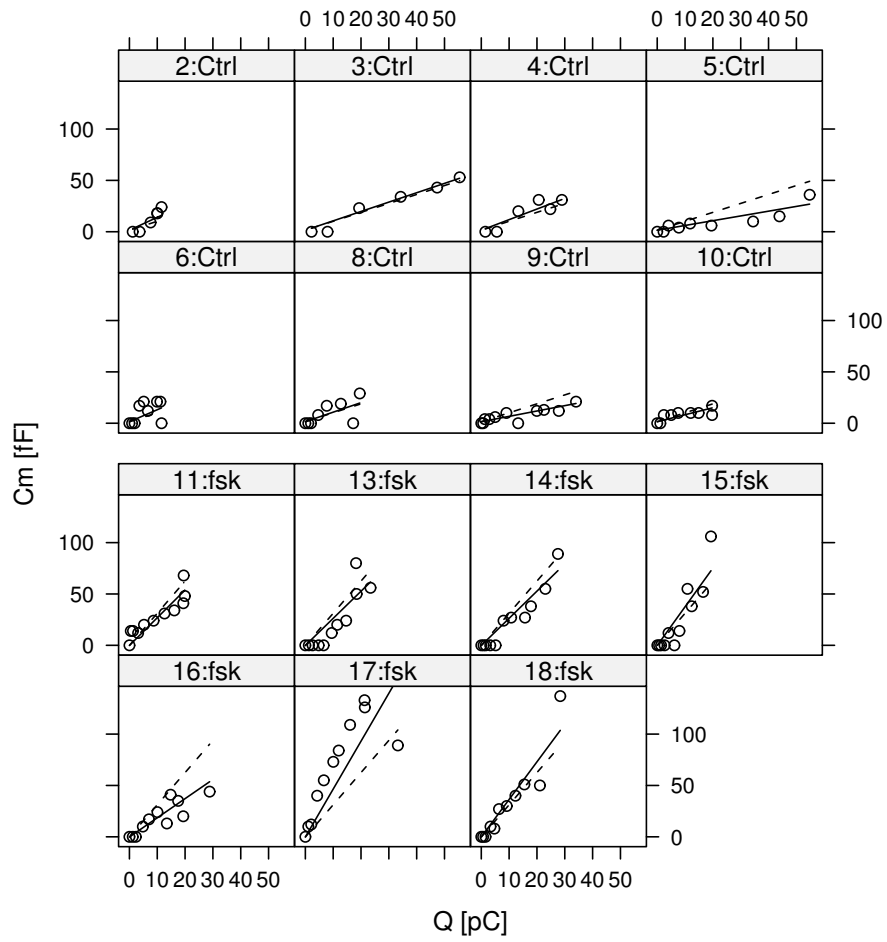
Figure 1: Mixed-effect analysis of ΔC_m versus Q in mouse β-cells. Panel names indicate cell number and group (Ctrl: control; fsk: 2 μM forskolin). Fits to the original data (circles) within each cell are given by the solid lines, while the dashed lines show the fit within each group.

the fact that the pancreas senses not only the plasma glucose concentration, but also how rapid the glucose concentration increases (Breda et al., 2001, 2002).

Other models describe the dynamics of granules as they move between different pools, and the control of exocytosis by Ca^{2+} (Bertuzzi et al., 2007; Chen et al., 2008; Pedersen and Sherman, 2009). Using such a model it was suggested (Pedersen and Sherman, 2009) that a highly Ca^{2+}-sensitive pool, described by capacitance measurements (Wan et al., 2004; Yang and Gillis, 2004) could correspond to newcomer granules seen in TIRF microscopy experiments (Ohara-Imaizumi et al., 2004), illustrating how mathematical models can be used to integrate data obtained with different techniques and on different timescales. This link between Ca^{2+}-sensitivity and fusion mode was partly confirmed experimentally (Ohara-Imaizumi et al., 2009).

A variation of these models was recently (Pedersen, 2010b) used to study the effect of palmitate exposure on Ca^{2+} and exocytosis (Hoppa et al., 2009). The question was whether palmitate disrupted Ca^{2+}-channel clustering or, possibly in addition, moved granules away from Ca^{2+}-channels. Modeling simulations showed that no clear conclusion could be drawn from capacitance measurements alone, but it was argued that imaging data (Hoppa et al., 2009) favored the interpretation that palmitate exposure dissociated granules from Ca^{2+}-channels.

3.3. Exocytosis in human β-cells

As outlined in the previous sections, rodent β-cells have been a subject of intense study, both experimentally and theoretically. However, the interest in rodent β-cells lies in the quest for understanding the defects in insulin secretion, and eventually for treatment and cure, of the *human* disease, diabetes mellitus. Thus, currently a major effort is devoted to the study of β-cells from human donors.

Human β-cells differ from their rodent counterparts in several aspects, for example with respect to their organization within the pancreatic islets (Brissova et al., 2005; Cabrera et al., 2006; Bosco et al., 2010) and the expression, regulation and role of various ion channels (Pressel and Misler, 1990; Barnett et al., 1995; Braun et al., 2008). The kinetics and control of exocytosis are also different. While short depolarizations (< 50 ms) are sufficient to trigger exocytosis in rodent β-cells (Barg et al., 2001; Eliasson et al., 2003; Wan et al., 2004; Vikman et al., 2006; Rose et al., 2007), longer depolarization (≥ 100 ms) are needed to evoke exocytosis in human β-cells

(Misler et al., 1992; Braun et al., 2008, 2009). Moreover, exocytosis stops immediately upon repolarization in rodent β-cells (Ammälä et al., 1993b; Eliasson et al., 2003; Wan et al., 2004), in contrast to the situation in human β-cells where the capacitance trace continues to increase after termination of the voltage pulse (Misler et al., 1992; Braun et al., 2008, 2009).

The long delay between Ca^{2+} influx and exocytosis in human β-cells suggests that the granules are located some distance away from the Ca^{2+}-channels, so that the delay is because of the time required for Ca^{2+} to diffuse to the exocytotic machinery. Alternatively, the delay in human β-cell exocytosis could be due to an inherent delay in the exocytotic process, which would show up as a delayed increase in capacitance after flash-release of caged-Ca^{2+}. Flash-release experiments have still not been performed in human β-cells, but we find it unlikely that they will reveal such long inherent delays, since exocytosis occurs < 15 ms after flash-release of caged-Ca^{2+} in other endocrine cells (Barg et al., 2001; Thomas et al., 1993; Heinemann et al., 1994).

We have developed a simple model of Ca^{2+}-dynamics and exocytosis in human β-cells. The cell is divided into five Ca^{2+}-compartments (Fig. 2): bulk cytosolic Ca^{2+} with concentration $[Ca^{2+}]_c$, denoted mathematically by Ca_i, a submembrane compartment with concentration $[Ca^{2+}]_{mem}$, denoted Ca_{mem}, and microdomains located below T-, L- and P/Q-type Ca^{2+}-channels. Calcium current of T-, L and P/Q-type are described as in a recent model of electrical activity in human β-cells (Pedersen, 2010a), and the resulting Ca^{2+}-flux is assumed to enter the corresponding microdomains. As in the analysis of the mouse data, we assume that microdomain Ca^{2+} is proportional to the corresponding types of Ca^{2+}-currents (Sherman et al., 1990) and is therefore not modeled explicitly. The submembrane compartment was distinguish from the general intracellular compartment in order to get a sufficiently rapid rise in the Ca^{2+}-concentration after the onset of the depolarization. In this way, a behavior resembling TIRFM-imaging of $[Ca^{2+}]_{mem}$ (Hoppa et al., 2009) was obtained. The Ca^{2+}-dynamics is described following (Chen et al., 2008; Pedersen and Sherman, 2009; Pedersen, 2010b), based on data from mouse β-cells (Chen et al., 2003). Exocytosis was assumed to be triggered from the submembrane Ca^{2+}-compartment, and its rate was modelled as a Hill-function of $[Ca^{2+}]_{mem}$ with relative high Ca^{2+}-sensitivity ($K_D = 2$ μM) and modest cooperativity ($n = 3$), mimicking the highly Ca^{2+}-sensitive pool described in rat β-cells (Wan et al., 2004). Motivated from the results of the analysis of mouse data in section 3.1, we assumed pool depletion not to occur.
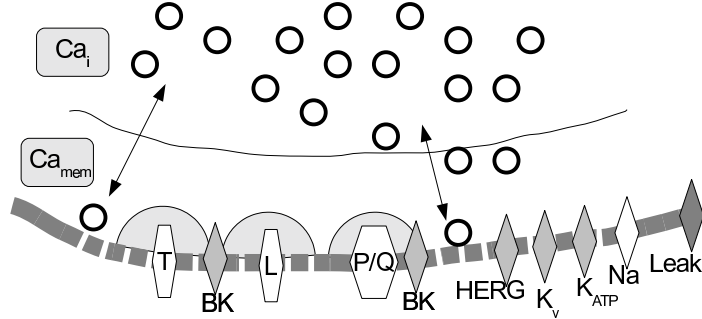
Figure 2: Overview of ion channels and granules in the model of human β-cells. Microdomain Ca^{2+} is supposed to be in equilibrium with the respective types of Ca^{2+}-currents, while the dynamics of $[Ca^{2+}]_{mem}$ and $[Ca^{2+}]_c$ are simulated.

All expressions and parameters can be found in the Methods section.

Simulations of a 500 ms depolarization, which triggers Ca^{2+}-currents (Fig. 3A), showed that the Ca^{2+}-concentrations in the submembrane compartment $[Ca^{2+}]_{mem}$ builds up slowly (Fig. 3B, full curve), as a result of the delay caused by diffusion. Because of the time required to reach triggering levels of $[Ca^{2+}]_{mem}$, virtually no exocytosis is seen until ~ 50 ms, whereafter exocytosis proceeds linearly as function of time (Fig. 3C, full curve), in good agreement with experimental data (Braun et al., 2008, 2009). After the voltage-clamp is returned to the holding potential of -70 mV, exocytosis proceeds for some time [Fig. 3C, full curve; Braun et al. (2008, 2009)] until $[Ca^{2+}]_{mem}$ has fallen sufficiently (Fig. 3B, full curve). Thus, the slow dynamics of $[Ca^{2+}]_{mem}$ gives rise to a delayed onset of exocytosis, and a continued increase in membrane capacitance after termination of the depolarizing pulse.

When L-type Ca^{2+}-channels are blocked, the onset of exocytosis is further delayed, but proceeds in parallel to the control case after this delay, both in the model (Fig. 3C, dotted curve) and in experiments (Braun et al., 2009). Moreover, as for the control case, exocytosis proceeds after the end of pulse (Fig. 3C, dotted curve) as observed experimentally (Braun et al., 2008). Because of their relatively fast inactivation kinetics, blockage of L-type Ca^{2+}-channels slows down the build-up of $[Ca^{2+}]_{mem}$, but has little effect of the level reached at the end of the 500 ms depolarization, which means that the dynamics of $[Ca^{2+}]_{mem}$ after termination of the pulse is similar to the control case (Fig. 3B). These facts explain the slower onset of exocytosis,

13

but unchanged post-depolarization capacitance increase.

In contrast, P/Q-type Ca^{2+}-channels inactivate very little during a 500 ms pulse (Braun et al., 2008), and are here assumed not to inactivate at all (Pedersen, 2010a). Therefore, antagonists of P/Q-channels will not only slow down the increase in $[Ca^{2+}]_{mem}$ during the first part of the depolarization, but will also lower $[Ca^{2+}]_{mem}$ through out the 500 ms pulse significantly (Fig. 3B, dashed curve). These changes lead to a delay in exocytosis, as well as a lower exocytotic rate after the onset, compared to the control case (Fig. 3C), in agreement with experiments (Braun et al., 2009). Moreover, exocytosis does not continue after repolarization when P/Q-type channels are blocked [Fig. 3C, dashed curve; Braun et al. (2008)]. Note that these results are not a consequence of closer association of P/Q-type channels to granules, compared to other Ca^{2+}-channel types, but is merely reflecting the major contribution of the P/Q-type Ca^{2+}-current to total Ca^{2+}-influx during a 500 ms depolarization caused by the much slower inactivation of P/Q-type channels compared to T- and L-type channels. During the last 300-400 ms of a 500 ms pulse, almost all Ca^{2+}-entry is through P/Q-type channels (Fig. 3A). Thus, blocking this channel type will lower $[Ca^{2+}]_{mem}$ much more than blocking any other Ca^{2+}-channel type (Fig. 3B), resulting in significantly less exocytosis (Fig. 3C), even though granules were not assumed to be located near P/Q-type Ca^{2+}-channels. To reproduce the experimental data (Braun et al., 2009), it was necessary to assume only partial ($\sim70\%$) block of the P/Q-type current, to allow some Ca^{2+}-influx even when T- and L-type channels had inactivated. This remaining Ca^{2+} flux could be due to voltage-dependent Ca^{2+}-channels not included in model (Braun et al., 2008), or to Ca^{2+}-induced Ca^{2+}-release from intracellular stores. Alternatively, it might simply be due to incomplete channel block. Indeed, the combined Ca^{2+}-channel antagonist-evoked reduction in Ca^{2+}-charge entry is only $\sim90\%$ (Braun et al., 2008).

To investigate the contribution of different Ca^{2+}-channel types during electrical activity, we imposed a voltage-trace simulated using a recent model (Pedersen, 2010a) on the exocytosis model described above. This allowed us to separate the effect of Ca^{2+}-channel blockage on electrical activity from its effect on exocytosis. We found that $[Ca^{2+}]_{mem}$ and exocytosis are lowered to a similar extent by blockage of either L- or P/Q-type channels (Fig. 4), both during spiking and rapid bursting electrical activity. In contrast with the response to the long (500 ms) depolarizations, L-type channels do not inactivate significantly during an action potential. Moreover, the action po-
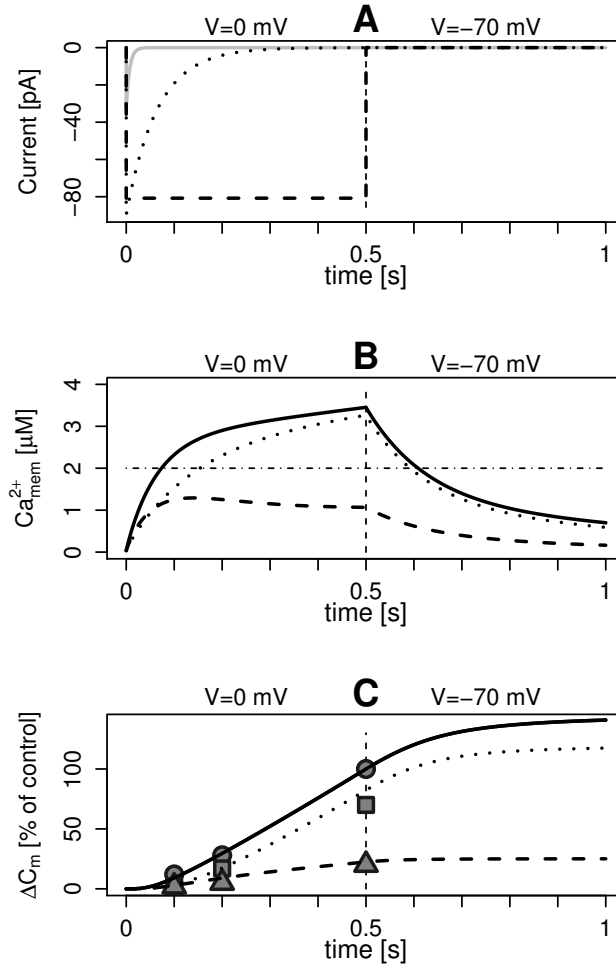
Figure 3: Ca^{2+}-currents and capacitance trace in response to a depolarization to 0 mV for 0.5 s in human β-cells reproducing results by Braun et al. (2009). A: Inactivation and magnitude of Ca^{2+}-currents of T- (grey), L- (dotted) and P/Q-type (dashed) were modeled as in Pedersen (2010a). B: Submembrane Ca^{2+}-concentration under control condition (full) or with blockage of L-type (dotted) or P/Q-type (70 % block; dashed) Ca^{2+}-channels. The horizontal dot-dashed line indicates the K_D-value of exocytosis of 2 μM. C: Cumulative capacitance change under control condition (full) or with blockage of L-type (dotted) or P/Q-type (dashed) Ca^{2+}-channels. Experimental data from Braun et al. (2009) are given for comparison under control conditions (circles), or in the presence of L-type (squares) or P/Q-type (triangles) antagonists. Capacitance increases have been scaled relative to the amount exocytosis evoked by a 500 ms depolarization under control conditions (Braun et al., 2009). In all panels, the vertical dashed lines indicates the end of the depolarization at 0.5 s after which the membrane potential was stepped back to -70 mV.

15

tentials peak at ≈ -10 mV, less than the 0 mV of imposed voltage-clamp depolarizations, which means that L-type, but not P/Q-type, channels get fully activated during electrical activity. This contributes to counteract the modest inactivation of L-type channels.

4. Conclusions

It is becoming evident that rodent and human β-cells differ in several aspects [see e.g. (Brissova et al., 2005; Braun et al., 2008)]. Mathematical modeling of electrical acitivity (Pedersen, 2010a) and exocytosis (subsection 3.3) in β-cells are beginning to take these differences into account. Such models based on human data will potentially be useful in the search for new anti-diabetic drugs, and for translating research performed on rodents to humans. Linking these cellular models to minimal models of insulin secretion (Breda et al., 2001), for example following Pedersen et al. (2010), might provide further insight in the pathophysiolology of diabetes.

Mathematical models of biological systems can be classified into two different groups, depending on their purpose (Cobelli et al., 2009). "Models-to-simulate" are detailed describtions of the biology based on biophysical, mechanistic hypotheses, while "models-to-measure" are used to extract otherwise unknown information, for example from exocytosis data (Chow et al., 1994; Pedersen, 2011). Such models are based on a simpler physiological description of the system under investigation, and the model complexity is minimal to assure more transparent conclusions. This latter modeling approach was used here for the study of exocytosis in human β-cells (subsection 3.3). The exocytosis model should be improved as new data emerges. In particular, studies of the Ca^{2+}-sensitivity using flash-release of caged-Ca^{2+} are needed. We showed that the 500 ms protocol often used to study exocytosis exaggerates the contribution from P/Q-type Ca^{2+}-channels due to their slow inactivation kinetics, and the model suggested that during electrical activity L- and P/Q-type Ca^{2+}-channels contribute to a similar degree to exocytosis. Thus, pulse protocols mimicking electrical activity better should preferably be applied when studying exocytosis in human β-cells.

The suggested loose coupling between Ca^{2+}-channels and releasable granules in human β-cells, and the resulting delayed and slow rate of release, is physiologically of little importance. Insulin targets tissues located far away from the β-cells, and the sub-second delay is therefore irrelevant compared to the time needed for transportation of insulin in the blood stream. Moreover,
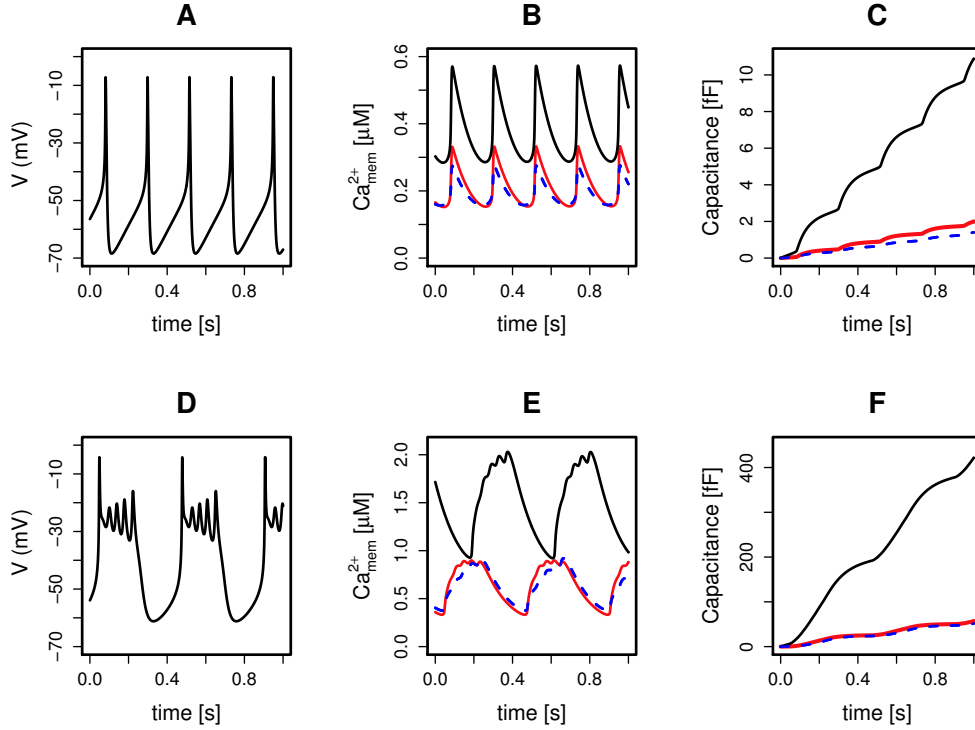
16

Figure 4: Similar contribution of L- and P/Q-type Ca^{2+}-channels to exocytosis during electrical activity in human β-cells. A: Spiking electrical activity simulated as in Fig. 2 of Pedersen (2010a) with the default parameters from Table 1 of that publication. B: Simulated $[Ca^{2+}]_{mem}$ with imposed spiking electrical activity (from panel A) under control condition (black curve), or with block of either P/Q-type (red curve) or L-type (blue, dashed curve) Ca^{2+}-channels in the model of Ca^{2+}-dynamics and exocytosis. C: Simulated capacitance increase resulting from exocytosis during spiking electrical activity under control condition (black curve), or with block of either P/Q-type (red curve) or L-type (blue, dashed curve) Ca^{2+}-channels in the model of Ca^{2+}-dynamics and exocytosis. D: Rapid bursting electrical activity simulated using the model from Pedersen (2010a) with its default parameters, except $g_{K(ATP)} = 0.010$ nS/pF and $V_{mKv} = 15$ mV. E: Simulated $[Ca^{2+}]_{mem}$ as in panel B, but during rapid bursting electrical activity. F: Simulated capacitance increase as in panel C, but during rapid bursting electrical activity.

insulin signaling in target tissues to modify glucose handling is a relatively slow process. In contrast, synaptic release must be fast since neurotransmitters signals to receptors located adjacent to the site of release and precise neuronal information transmission is crucial. On the contrary, a loose coupling could have the advantage that erratic action potentials will not lead to exocytosis, but only episodes of more intense electrical activity in response to elevated plasma glucose levels will allow $[Ca^{2+}]_{mem}$ to build-up sufficiently to trigger release, in this way reducing basal secretion during periods of fasting.

We performed a careful reanalysis of previously published data on the Ca^{2+}-control of exocytosis in mouse β-cells (Eliasson et al., 2003) using a mixed-effects model to take into consideration within-cell correlation and between-cell variation. The performed data-analysis is a good example of how a minimal "model-to-measure" (Pedersen, 2011) allowed insight to be obtained from a statistical analysis. Our results (subsection 3.1) revealed no substantial pool depletion since the relationship between capacitance increase and Ca^{2+}-entry was linear, suggesting that the IRP constitutes most of the RRP in mouse β-cells. In intact mouse islets, exocytosis in β-cells shows no sign of pool depletion (Göpel et al., 2004) in line with our finding. Also, human β-cell-exocytosis does not plateau for depolarizations up to 500 ms (Braun et al., 2008, 2009), again arguing against pool depletion. However, this does not means that depletion of the RRP is irrelevant for biphasic insulin secretion, indeed there is good evidence for a role of a finite pool of granules (Daniel et al., 1999; Henquin et al., 2002; Olofsson et al., 2002), but rather that short depolarizations of increasing lengths do not show evidence of a smaller IRP. Finally, our results confirmed that cAMP-raising agents such as forskolin increase the efficacy of Ca^{2+} on exocytosis.

Acknowledgements

References

Ammälä, C., Ashcroft, F. M., Rorsman, P., May 1993a. Calcium-independent potentiation of insulin release by cyclic AMP in single beta-cells. Nature 363 (6427), 356–358.

Ammälä, C., Eliasson, L., Bokvist, K., Larsson, O., Ashcroft, F. M., Rorsman, P., Dec 1993b. Exocytosis elicited by action potentials and voltage-clamp calcium currents in individual mouse pancreatic B-cells. J Physiol 472, 665–688.

Ashcroft, F. M., Rorsman, P., 1989. Electrophysiology of the pancreatic β-cell. Prog. Biophys. Mol. Biol. 54, 87–143.

Augustine, G. J., Adler, E. M., Charlton, M. P., 1991. The calcium signal for transmitter secretion from presynaptic nerve terminals. Ann N Y Acad Sci 635, 365–381.

Barg, S., Ma, X., Eliasson, L., Galvanovskis, J., Göpel, S. O., Obermüller, S., Platzer, J., Renström, E., Trus, M., Atlas, D., Striessnig, J., Rorsman, P., Dec 2001. Fast exocytosis with few Ca(2+) channels in insulin-secreting mouse pancreatic B cells. Biophys J 81 (6), 3308–3323.

Barnett, D. W., Pressel, D. M., Misler, S., Dec 1995. Voltage-dependent Na+ and Ca2+ currents in human pancreatic islet beta-cells: evidence for roles in the generation of action potentials and insulin secretion. Pflugers Arch 431 (2), 272–282.

Bertuzzi, A., Salinari, S., Mingrone, G., Jul 2007. Insulin granule trafficking in beta-cells: mathematical model of glucose-induced insulin secretion. Am J Physiol Endocrinol Metab 293 (1), E396–E409.

Bosco, D., Armanet, M., Morel, P., Niclauss, N., Sgroi, A., Muller, Y. D., Giovannoni, L., Parnaud, G., Berney, T., May 2010. Unique arrangement of alpha- and beta-cells in human islets of langerhans. Diabetes 59 (5), 1202–1210.

Brandt, A., Khimich, D., Moser, T., Dec 2005. Few CaV1.3 channels regulate the exocytosis of a synaptic vesicle at the hair cell ribbon synapse. J Neurosci 25 (50), 11577–11585.

Braun, M., Ramracheya, R., Bengtsson, M., Zhang, Q., Karanauskaite, J., Partridge, C., Johnson, P. R., Rorsman, P., Jun 2008. Voltage-gated ion channels in human pancreatic beta-cells: electrophysiological characterization and role in insulin secretion. Diabetes 57 (6), 1618–1628.

Braun, M., Ramracheya, R., Johnson, P. R., Rorsman, P., Jan 2009. Exocytotic properties of human pancreatic beta-cells. Ann N Y Acad Sci 1152, 187–193.

Breda, E., Cavaghan, M. K., Toffolo, G., Polonsky, K. S., Cobelli, C., Jan 2001. Oral glucose tolerance test minimal model indexes of beta-cell function and insulin sensitivity. Diabetes 50 (1), 150–158.

Breda, E., Toffolo, G., Polonsky, K. S., Cobelli, C., Feb 2002. Insulin release in impaired glucose tolerance: oral minimal model predicts normal sensitivity to glucose but defective response times. Diabetes 51 Suppl 1, S227–S233.

Brissova, M., Fowler, M. J., Nicholson, W. E., Chu, A., Hirshberg, B., Harlan, D. M., Powers, A. C., 2005. Assessment of human pancreatic islet architecture and composition by laser scanning confocal microscopy. J. Histochem. Cytochem. 53, 1087–1097.

Cabrera, O., Berman, D. M., Kenyon, N. S., Ricordi, C., Berggren, P.-O., Caicedo, A., 2006. The unique cytoarchitecture of human pancreatic islets has implications for islet cell function. Proc. Natl. Acad. Sci. 103, 2334–2339.

Chen, L., Koh, D. S., Hille, B., 2003. Dynamics of calcium clearance in mouse pancreatic β-cells. Diabetes 52, 1723–1731.

Chen, Y., Wang, S., Sherman, A., Sep 2008. Identifying the targets of the amplifying pathway for insulin secretion in pancreatic beta-cells by kinetic modeling of granule exocytosis. Biophys J 95 (5), 2226–2241.

Chow, R. H., Klingauf, J., Neher, E., Dec 1994. Time course of ca2+ concentration triggering exocytosis in neuroendocrine cells. Proc Natl Acad Sci U S A 91 (26), 12765–12769.

Cobelli, C., Dalla Man, C., Sparacino, G., Magni, L., De Nicolao, G., Kovatchev, B. P., 2009. Diabetes: Models, signals, and control. IEEE Reviews in Biomedical Engineering 2, 54–96.

Curry, D. L., Bennett, L. L., Grodsky, G. M., Sep 1968. Dynamics of insulin secretion by the perfused rat pancreas. Endocrinology 83 (3), 572–584.

Daniel, S., Noda, M., Straub, S. G., Sharp, G. W., Sep 1999. Identification of the docked granule pool responsible for the first phase of glucose-stimulated insulin secretion. Diabetes 48 (9), 1686–1690.

De Schutter, E., Smolen, P., 1998. Calcium dynamics in large neuronal models. In: Koch, C., Segev, I. (Eds.), Methods in neuronal modeling: from ions to networks, 2nd Edition. MIT Press, Cambridge, MA, USA, Ch. 6.

Ding, W. G., Gromada, J., Apr 1997. Protein kinase A-dependent stimulation of exocytosis in mouse pancreatic beta-cells by glucose-dependent insulinotropic polypeptide. Diabetes 46 (4), 615–621.

Eliasson, L., Abdulkader, F., Braun, M., Galvanovskis, J., Hoppa, M. B., Rorsman, P., Jul 2008. Novel aspects of the molecular mechanisms controlling insulin secretion. J Physiol 586 (14), 3313–3324.

Eliasson, L., Ma, X., Renström, E., Barg, S., Berggren, P.-O., Galvanovskis, J., Gromada, J., Jing, X., Lundquist, I., Salehi, A., Sewing, S., Rorsman, P., Mar 2003. SUR1 regulates PKA-independent cAMP-induced granule priming in mouse pancreatic B-cells. J Gen Physiol 121 (3), 181–197.

Eliasson, L., Renström, E., Ding, W. G., Proks, P., Rorsman, P., Sep 1997. Rapid ATP-dependent priming of secretory granules precedes Ca(2+)-induced exocytosis in mouse pancreatic B-cells. J Physiol 503 (Pt 2), 399–412.

Engisch, K. L., Nowycky, M. C., Feb 1996. Calcium dependence of large dense-cored vesicle exocytosis evoked by calcium influx in bovine adrenal chromaffin cells. J Neurosci 16 (4), 1359–1369.

Ermentrout, G., 2002. Simulating, analyzing, and animating dynamical systems: A guide to XPPAUT for researchers and students. SIAM Books, Philadelphia.

Fujimoto, K., Shibasaki, T., Yokoi, N., Kashima, Y., Matsumoto, M., Sasaki, T., Tajima, N., Iwanaga, T., Seino, S., Dec 2002. Piccolo, a Ca2+ sensor in pancreatic beta-cells. involvement of cAMP-GEFII.Rim2.Piccolo complex in cAMP-dependent exocytosis. J Biol Chem 277 (52), 50497–50502.

Gembal, M., Gilon, P., Henquin, J. C., 1992. Evidence that glucose can control insulin release independently from its action on ATP-sensitive K+ channels in mouse B cells. J Clin Invest 89 (4), 1288–95.

Gillis, K. D., Misler, S., Jan 1992. Single cell assay of exocytosis from pancreatic islet B cells. Pflugers Arch 420 (1), 121–123.

Gillis, K. D., Misler, S., Jul 1993. Enhancers of cytosolic cAMP augment depolarization-induced exocytosis from pancreatic B-cells: evidence for effects distal to Ca2+ entry. Pflugers Arch 424 (2), 195–197.

Göpel, S., Zhang, Q., Eliasson, L., Ma, X.-S., Galvanovskis, J., Kanno, T., Salehi, A., Rorsman, P., May 2004. Capacitance measurements of exocytosis in mouse pancreatic alpha-, beta- and delta-cells within intact islets of langerhans. J Physiol 556 (Pt 3), 711–726.

Grodsky, G. M., 1972. A threshold distribution hypothesis for packet storage of insulin and its mathematical modeling. J. Clin. Invest. 51, 2047–2059.

Gromada, J., Bokvist, K., Ding, W. G., Holst, J. J., Nielsen, J. H., Rorsman, P., Jan 1998. Glucagon-like peptide 1 (7-36) amide stimulates exocytosis in human pancreatic beta-cells by both proximal and distal regulatory steps in stimulus-secretion coupling. Diabetes 47 (1), 57–65.

Heinemann, C., Chow, R. H., Neher, E., Zucker, R. S., Dec 1994. Kinetics of the secretory response in bovine chromaffin cells following flash photolysis of caged Ca2+. Biophys J 67 (6), 2546–2557.

Henquin, J.-C., 2000. Triggering and amplifying pathways of regulation of insulin secretion by glucose. Diabetes 49, 1751–1760.

Henquin, J.-C., Ishiyama, N., Nenquin, M., Ravier, M. A., Jonas, J.-C., Feb 2002. Signals and pools underlying biphasic insulin secretion. Diabetes 51 Suppl 1, S60–S67.

Hoppa, M. B., Collins, S., Ramracheya, R., Hodson, L., Amisten, S., Zhang, Q., Johnson, P., Ashcroft, F. M., Rorsman, P., Dec 2009. Chronic palmitate exposure inhibits insulin secretion by dissociation of Ca(2+) channels from secretory granules. Cell Metab 10 (6), 455–465.

Horrigan, F. T., Bookman, R. J., Nov 1994. Releasable pools and the kinetics of exocytosis in adrenal chromaffin cells. Neuron 13 (5), 1119–1129.

Hosker, J. P., Rudenski, A. S., Burnett, M. A., Matthews, D. R., Turner, R. C., Aug 1989. Similar reduction of first- and second-phase B-cell responses at three different glucose levels in type II diabetes and the effect of gliclazide therapy. Metabolism 38 (8), 767–772.

Ivarsson, R., Jing, X., Waselle, L., Regazzi, R., Renström, E., Nov 2005. Myosin 5a controls insulin granule recruitment during late-phase secretion. Traffic 6 (11), 1027–1035.

Ivarsson, R., Obermüller, S., Rutter, G. A., Galvanovskis, J., Renström, E., Oct 2004. Temperature-sensitive random insulin granule diffusion is a prerequisite for recruiting granules for release. Traffic 5 (10), 750–762.

Jonkers, F. C., Henquin, J.-C., 2001. Measurements of cytoplasmic Ca^{2+} in islet cell clusters show that glucose rapidly recruits beta-cells and gradually increases the individual cell response. Diabetes 50, 540–550.

Klingauf, J., Neher, E., Feb 1997. Modeling buffered ca2+ diffusion near the membrane: implications for secretion in neuroendocrine cells. Biophys J 72 (2 Pt 1), 674–690.

Lindau, M., Neher, E., Feb 1988. Patch-clamp techniques for time-resolved capacitance measurements in single cells. Pflugers Arch 411 (2), 137–146.

Maechler, P., Wollheim, C. B., Dec 1999. Mitochondrial glutamate acts as a messenger in glucose-induced insulin exocytosis. Nature 402 (6762), 685–9.

Misler, S., Barnett, D. W., Gillis, K. D., Pressel, D. M., Oct 1992. Electrophysiology of stimulus-secretion coupling in human beta-cells. Diabetes 41 (10), 1221–1228.

Moser, T., Neher, E., Apr 1997. Rapid exocytosis in single chromaffin cells recorded from mouse adrenal slices. J Neurosci 17 (7), 2314–2323.

Ohara-Imaizumi, M., Aoyagi, K., Nakamichi, Y., Nishiwaki, C., Sakurai, T., Nagamatsu, S., Jul 2009. Pattern of rise in subplasma membrane Ca2+ concentration determines type of fusing insulin granules in pancreatic beta cells. Biochem Biophys Res Commun 385 (3), 291–295.

Ohara-Imaizumi, M., Nishiwaki, C., Kikuta, T., Nagai, S., Nakamichi, Y., Nagamatsu, S., Jul 2004. TIRF imaging of docking and fusion of single insulin granule motion in primary rat pancreatic beta-cells: different behaviour of granule motion between normal and Goto-Kakizaki diabetic rat beta-cells. Biochem J 381 (Pt 1), 13–18.

Olofsson, C. S., Göpel, S. O., Barg, S., Galvanovskis, J., Ma, X., Salehi, A., Rorsman, P., Eliasson, L., May 2002. Fast insulin secretion reflects exocytosis of docked granules in mouse pancreatic B-cells. Pflugers Arch 444 (1-2), 43–51.

Ozaki, N., Shibasaki, T., Kashima, Y., Miki, T., Takahashi, K., Ueno, H., Sunaga, Y., Yano, H., Matsuura, Y., Iwanaga, T., Takai, Y., Seino, S., Nov 2000. cAMP-GEFII is a direct target of cAMP in regulated exocytosis. Nat Cell Biol 2 (11), 805–811.

Pedersen, M. G., Nov 2010a. A biophysical model of electrical activity in human β-cells. Biophys J 99 (10), 3200–3207.

Pedersen, M. G., Dec 2010b. Insulin secretory granules enter a highly calcium-sensitive state following palmitate-induced dissociation from calcium channels: a theoretical study. J Neuroendocrinol 22 (12), 1315–1324.

Pedersen, M. G., 2010c. Pharmacological effects on insulin release in a mathematical model of human beta cells. Diabetologia 53, Suppl 1, S223.

Pedersen, M. G., 2011. On depolarization-evoked exocytosis as a function of calcium entry: possibilities and pitfalls. Biophys J. In Press.

Pedersen, M. G., Corradin, A., Toffolo, G. M., Cobelli, C., Oct 2008. A subcellular model of glucose-stimulated pancreatic insulin secretion. Philos Transact A Math Phys Eng Sci 366 (1880), 3525–3543.

Pedersen, M. G., Sherman, A., May 2009. Newcomer insulin secretory granules as a highly calcium-sensitive pool. Proc Natl Acad Sci U S A 106 (18), 7432–7436.

Pedersen, M. G., Toffolo, G. M., Cobelli, C., Mar 2010. Cellular modeling: insight into oral minimal models of insulin secretion. Am J Physiol Endocrinol Metab 298 (3), E597–E601.

Pinheiro, J. C., Bates, D. M., 2000. Mixed-Effects Models in S and S-PLUS. Springer, New York.

Prentki, M., Vischer, S., Glennon, M. C., Regazzi, R., Deeney, J. T., Corkey, B. E., Mar 1992. Malonyl-CoA and long chain acyl-CoA esters as metabolic coupling factors in nutrient-induced insulin secretion. J Biol Chem 267 (9), 5802–10.

Pressel, D. M., Misler, S., Jul 1990. Sodium channels contribute to action potential generation in canine and human pancreatic islet B cells. J Membr Biol 116 (3), 273–280.

Proks, P., Eliasson, L., Ammälä, C., Rorsman, P., Ashcroft, F. M., Oct 1996. Ca(2+)- and GTP-dependent exocytosis in mouse pancreatic beta-cells involves both common and distinct steps. J Physiol 496 (Pt 1), 255–264.

Renström, E., Eliasson, L., Bokvist, K., Rorsman, P., Jul 1996. Cooling inhibits exocytosis in single mouse pancreatic B-cells by suppression of granule mobilization. J Physiol 494 (Pt 1), 41–52.

Renström, E., Eliasson, L., Rorsman, P., Jul 1997. Protein kinase A-dependent and -independent stimulation of exocytosis by cAMP in mouse pancreatic B-cells. J Physiol 502 (Pt 1), 105–118.

Rose, T., Efendic, S., Rupnik, M., Jun 2007. Ca2+-secretion coupling is impaired in diabetic Goto Kakizaki rats. J Gen Physiol 129 (6), 493–508.

Sherman, A., Keizer, J., Rinzel, J., Oct 1990. Domain model for ca2(+)-inactivation of ca2+ channels at low channel density. Biophys J 58 (4), 985–995.

Smith, P. A., Duchen, M. R., Ashcroft, F. M., Sep 1995. A fluorimetric and amperometric study of calcium and secretion in isolated mouse pancreatic beta-cells. Pflugers Arch 430 (5), 808–818.

Thomas, P., Wong, J. G., Lee, A. K., Almers, W., Jul 1993. A low affinity Ca2+ receptor controls the final steps in peptide secretion from pituitary melanotrophs. Neuron 11 (1), 93–104.

Varadi, A., Ainscow, E. K., Allan, V. J., Rutter, G. A., Apr 2002. Molecular mechanisms involved in secretory vesicle recruitment to the plasma membrane in beta-cells. Biochem Soc Trans 30 (2), 328–332.

Venables, W. N., Ripley, B. D., 2002. Modern Applied Statistics with S, 4th Edition. Springer, New York.

Vikman, J., Ma, X., Hockerman, G. H., Rorsman, P., Eliasson, L., Jun 2006. Antibody inhibition of synaptosomal protein of 25 kDa (SNAP-25) and syntaxin 1 reduces rapid exocytosis in insulin-secreting cells. J Mol Endocrinol 36 (3), 503–515.

Vikman, J., Svensson, H., Huang, Y.-C., Kang, Y., Andersson, S. A., Gaisano, H. Y., Eliasson, L., Aug 2009. Truncation of SNAP-25 reduces the stimulatory action of cAMP on rapid exocytosis in insulin-secreting cells. Am J Physiol Endocrinol Metab 297 (2), E452–E461.

Wan, Q.-F., Dong, Y., Yang, H., Lou, X., Ding, J., Xu, T., Dec 2004. Protein kinase activation increases insulin secretion by sensitizing the secretory machinery to Ca2+. J Gen Physiol 124 (6), 653–662.

Wiser, O., Trus, M., Hernández, A., Renström, E., Barg, S., Rorsman, P., Atlas, D., Jan 1999. The voltage sensitive Lc-type Ca2+ channel is functionally coupled to the exocytotic machinery. Proc Natl Acad Sci U S A 96 (1), 248–253.

Yang, Y., Gillis, K. D., Dec 2004. A highly Ca2+-sensitive pool of granules is regulated by glucose and protein kinases in insulin-secreting INS-1 cells. J Gen Physiol 124 (6), 641–651.